ROLLING MOMENT DERIVATIVE, L_ξ, FOR PLAIN AILERONS AT SUBSONIC SPEEDS

1. NOTATION AND UNITS

		SI	*British*
A	aspect ratio		
$(a_1)_0$	section lift-curve slope with incidence in incompressible flow	rad^{-1}	rad^{-1}
$(a_2)_0$	section lift-curve slope with control deflection in incompressible flow	rad^{-1}	rad^{-1}
b	wing span	m	ft
C_L	lift coefficient, $L/½\rho V^2 S$		
C_l	rolling moment coefficient $\mathscr{L}/½\rho V^2 Sb$		
c_f/c	ratio of aileron chord aft of hinge line to local wing chord, at mid-span of aileron		
K_1	value of Φ_ξ for rectangular wing		
K_2	secondary planform component of Φ_ξ		
k_1	correction factor for wing thickness		
k_2	correction factor for Reynolds number		
L	lift	N	lbf
$\mathscr{L}$	rolling moment	N m	lbf ft
L_ξ	rolling moment derivative with respect to ξ, $\partial C_l/\partial\xi$	rad^{-1}	rad^{-1}
$L_{\xi'}$	rolling moment derivative with respect to ξ', $\partial C_l/\partial\xi'$	rad^{-1}	rad^{-1}
M	free-stream Mach number		
R	Reynolds number based on aerodynamic mean chord of wing		
S	wing planform area	m^2	ft^2
s	wing semispan	m	ft
t/c	section thickness to chord ratio of wing at mid-span of aileron		

Issued August 1988
With Amendments A and B, October 1992

V	free-stream velocity	m/s	ft/s
α	incidence	rad	rad
β	compressibility parameter, $(1 - M^2)^{1/2}$		
δ	deflection angle of full-span plain control measured in plane parallel to plane of symmetry, positive for trailing-edge down	rad	rad
η	spanwise distance from wing centre-line as fraction of semispan		
η_i	value of η at inboard limit of aileron at hinge line		
η_o	value of η at outboard limit of aileron at hinge line		
$\bar{\eta}$	$(\eta_i + \eta_o)/2$		
λ	wing taper, ratio of tip chord to centre-line chord		
$\Lambda_{1/2}$	sweepback of wing mid-chord line	deg	deg
Λ_h	sweepback of aileron hinge line	deg	deg
ξ	aileron deflection angle measured in plane parallel to plane of symmetry, arithmetic mean of deflection angles of port and starboard ailerons, positive for starboard aileron down and port aileron up	rad	rad
ξ'	aileron deflection angle measured in plane normal to hinge line, $\tan^{-1}(\tan\xi \sec\Lambda_h)$	rad	rad
ρ	density of air	kg/m^3	slug/ft^3
τ	section trailing-edge angle at mid-span of aileron	deg	deg
Φ	part-span lift correction function in Item No. 74012 (Derivation 5), ratio of lift coefficient increment due to flaps of span $b\eta$ extending symmetrically about wing centre-line to lift coefficient increment due to full-span flaps at same deflection		
Φ_ξ	aileron rolling moment correction function, see Section 2.3 and Equation (2.5)		
$\Phi_{\xi i}$	value of Φ_ξ for $\eta = \eta_i$		
$\Phi_{\xi o}$	value of Φ_ξ for $\eta = \eta_o$		

Subscripts

T	denotes theoretical value
$t = 0$	denotes value for section of zero thickness

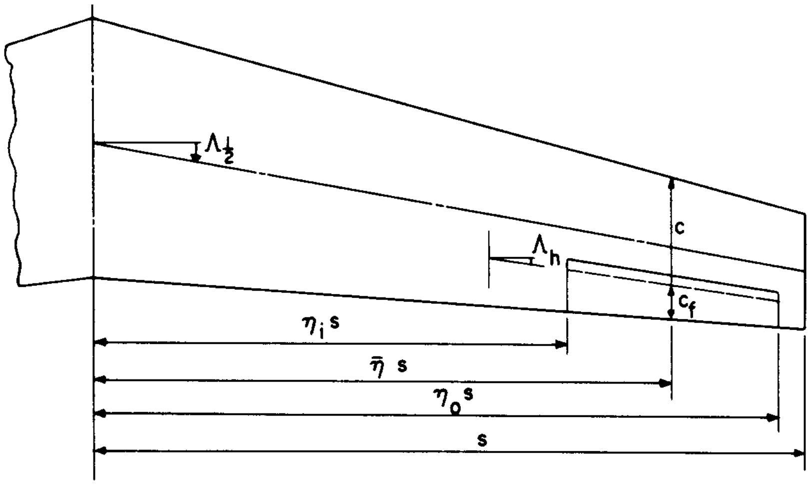

Sketch 1.1 Wing and aileron geometry

2. METHOD*

This Item presents a semi-empirical method for predicting the rolling moment derivative due to the operation of plain sealed aileron controls for attached flow at subsonic speeds. The method combines a geometrically defined moment arm $\bar{\eta}$ with a full-span control deflection characteristic $\partial C_L/\partial\delta$ that is modified by a correction function $(\Phi_{\xi i}-\Phi_{\xi o})$ that allows for the part-span of the ailerons and their effectiveness in producing rolling moment. The derivative for antisymmetric deflection of the ailerons is given by the equation

$$L_\xi = -\tfrac{1}{2}\bar{\eta}(\partial C_L/\partial\delta)(\Phi_{\xi i}-\Phi_{\xi o}), \tag{2.1}$$

where the aileron deflection angle is ξ, measured in a plane parallel to the plane of symmetry.

If the aileron deflection angle is ξ', measured in a plane normal to the hinge line, the corresponding derivative is

$$L_{\xi'} = L_\xi \cos\Lambda_h, \tag{2.2}$$

where Λ_h is the sweepback of the aileron hinge line.

2.1 Moment Arm

In Equation (2.1), $\bar{\eta}$ approximates to the spanwise moment arm of each aileron expressed as a fraction of the semispan s. It is taken as

$$\bar{\eta} = \tfrac{1}{2}(\eta_i+\eta_o), \tag{2.3}$$

* A FORTRAN computer program is available for the method of this Item and that of Item No. 88029 as ESDUpac A8840, see Item No. 88040 for details.

the mean of the aileron inboard and outboard limits measured at the hinge line. This simple geometric definition neglects the effect of wing taper, but this is small for practical aileron spans $(\eta_o - \eta_i \le 0.4s)$.

An extra factor of ½ appears in Equation (2.1) because the rolling moment coefficient is based on a reference length equal to the full span b.

2.2 Plain Control Derivative

The derivative $\partial C_L / \partial\delta$ in Equation (2.1) is the rate of change of lift coefficient due to control deflection for full-span plain controls, as predicted by the method in Item No. 74011 (Derivation 4), where it is presented in terms of the theoretical wing lift-curve slope $[\partial C_L/\partial\alpha]_T$, wing and control geometry, Reynolds number and Mach number in the form

$$\frac{\partial C_L}{\partial\delta} = \left[\frac{\partial C_L}{\partial\delta} \Big/ \frac{\partial C_L}{\partial\alpha}\right]_T \left[\frac{\partial C_L}{\partial\alpha}\right]_T [1 - k_1 k_2] \,. \tag{2.4}$$

The first expression in brackets on the right hand side of the equation is given in Figure 1 as a carpet in terms of $1/\beta A$ and c_f/c. The second expression in brackets is evaluated using Item No. 70011 (Derivation 3) which gives $[\partial C_L/\partial\alpha]_T/A$ in terms of λ, βA and $A\tan\Lambda_{1/2}$. The factors k_1 and k_2 appearing in the third expression in brackets are given in Figures 2 and 3; k_1 corrects for section thickness and is given in terms of $(t/c)\sec\Lambda_{1/2}$ and c_f/c, and k_2 corrects for Reynolds number and is given in terms of $\log_{10}R$ and c_f/c. Although the methods in Item Nos 74011 and 70011 are presented for wing planform parameters under the assumption of straight taper, they may be used for other planforms by employing the geometric technique in Appendix A of Item No. 76003 (Derivation 6) to construct an “equivalent” straight-tapered wing to provide suitably representative values of λ, A and $A\tan\Lambda_{1/2}$.

The data in Figures 1 to 3 have been reproduced directly from Item No. 74011 to avoid cross referencing. Values of c_f/c and t/c appropriate to the mid-span of the aileron should be taken. In the original construction of the correction factors k_1 and k_2 it was assumed that the section geometry was such that $\tau = 100\ t/c$ (degrees). If τ lies outside the range $50t/c \le \tau \le 150t/c$ it is necessary to use Item Nos Aero W.01.01.05 (Derivation 1) and Aero C.01.01.03 (Derivation 2) to calculate the necessary section properties and replace the term $[1 - k_1k_2]$ by its full form $[(a_2)_0/(a_2)_{0\ T\ t=0}]/[(a_1)_0/2\pi]$, with t/c and τ measured in a plane normal to the wing mid-chord sweep line.

2.3 Rolling Moment Correction Factors

The term $(\Phi_{\xi i} - \Phi_{\xi o})$ in Equation (2.1) allows for the finite span of the ailerons and for their effectiveness in producing rolling moment. Calculation of $\Phi_{\xi i}$ and $\Phi_{\xi o}$ is carried out by evaluating the correction function Φ_ξ at $\eta = \eta_i$ and $\eta = \eta_o$ respectively. The function Φ_ξ is expressed in terms of a value K_1 appropriate to a rectangular wing, from which is subtracted a secondary planform component, K_2, so that

$$\Phi_\xi = K_1 - K_2 \,. \tag{2.5}$$

Figure 4a gives K_1 as a carpet in η and $1/\beta A$ for $0 \le \eta \le 1$ and $0 \le 1/\beta A \le 0.5$. Figures 4b and 4c show, for $0.08 \le 1/\beta A \le 0.30$, the central part of the carpet on an expanded scale. Figure 5 gives K_2 as a function of η for a series of values of the planform parameter $A\ \tan\Lambda_{1/2} - 8\lambda$.

The functions K_1 and K_2 have been established by analysing the wind-tunnel data on rolling moment in Derivations 7 to 39, and by making use of some of the results in Item No. 74012 (Derivation 5) which gives a function Φ for converting the lift coefficient increment due to full-span flaps to that for symmetrically deflected part-span flaps that extend equally to each side of the wing centre-line. Data from tests on half-wing models have been excluded from the analysis because of the large correction factors that are applied to rolling moments measured in such tests.

It has been found that for wings of high aspect ratio ($1/\beta A \le 0.08$) K_1 depends only on η and K_2 varies with $A \tan\Lambda_{1/2} - 8\lambda$ as in Item No 74012. For lower aspect ratios the same assumption has been made for K_2, and the general variation of the function K_1 has been found by correlating the quantity L_ξ *(experiment)*$/[-\frac{1}{2}\bar{\eta}(\partial C_L/\partial\delta)] + K_2$ for outboard ailerons in terms of η_i and $1/\beta A$. Figures 4a to 4c represent the result of this analysis; dashed areas of the carpets indicate the lack of experimental data. Comparisons with experimental data for inboard ailerons show that the method remains sound.

Figure 4a has been constructed mainly from an analysis of data from low speed tests, $M \le 0.6$, but its applicability has been extended by using the similarity parameter $1/\beta A$ as a variable rather than $1/A$. Comparisons with a limited number of data from high speed tests (Derivations 12, 13, 15 and 28) show that satisfactory estimates of L_ξ can be obtained up to about $M = 0.8$ to 0.85. See also the comments in Section 4.

3. AILERON LIFT CHARACTERISTICS

Equation (2.1) must only be used in the calculation of the rolling moment derivative L_ξ, as it has been determined empirically solely for this purpose. The moment arm $\bar{\eta}$ is too approximate for that equation to be used to infer the lift-curve slope due to control deflection for individual ailerons. If required, the aileron lift-curve slope should be obtained by using the full-span control characteristic predicted by Item No. 74011 (Derivation 4) in conjunction with the part-span correction provided by Item No. 74012 (Derivation 5).

4. ACCURACY AND APPLICABILITY

Predicted and experimental values of L_ξ are compared in Sketch 4.1. In general, L_ξ is predicted to within about $\pm 20\%$ up to $L_\xi \approx -0.15$ and to within about ± 0.03 thereafter. The analysis has been confined to ranges of ξ ($\le \pm 10^\circ$ say) over which the variation of the rolling moment coefficient is essentially linear, and to low angles of incidence, although there is usually only a slow reduction in the magnitude of L_ξ up to $\alpha \approx 10°$.

Table 4.1 shows the ranges of model geometry and flow parameters covered in the analysis. The ratio of control chord to wing chord and section properties are assumed to be fairly constant across the span of the aileron, and modest departures are compensated by defining c_f/c, t/c and τ at the mid-span of the aileron.

Attention has been restricted to ailerons that are effectively sealed. There will be a reduction in aileron effectiveness if there is flow through a control gap. If the aileron is nose-balanced rather than plain, the effect is to extend the range over which the rolling moment coefficient is linear with ξ, but the derivative L_ξ should remain essentially the same. The methods in Item Nos 70011 and 74011 assume that the flow over the wing is wholly subsonic and fully attached, and so the same restrictions apply to the method of this Item.

TABLE 4.1

Parameter	*Range*	*Parameter*	*Range*
A	2 to 12	τ	7° to 16°
$\Lambda_{1/2}$	0 to 60°	c_f/c	0.15 to 0.35
λ	0.2 to 1	M	0 to 0.85
t/c	0.06 to 0.15	R	0.6×10^6 to 8×10^6

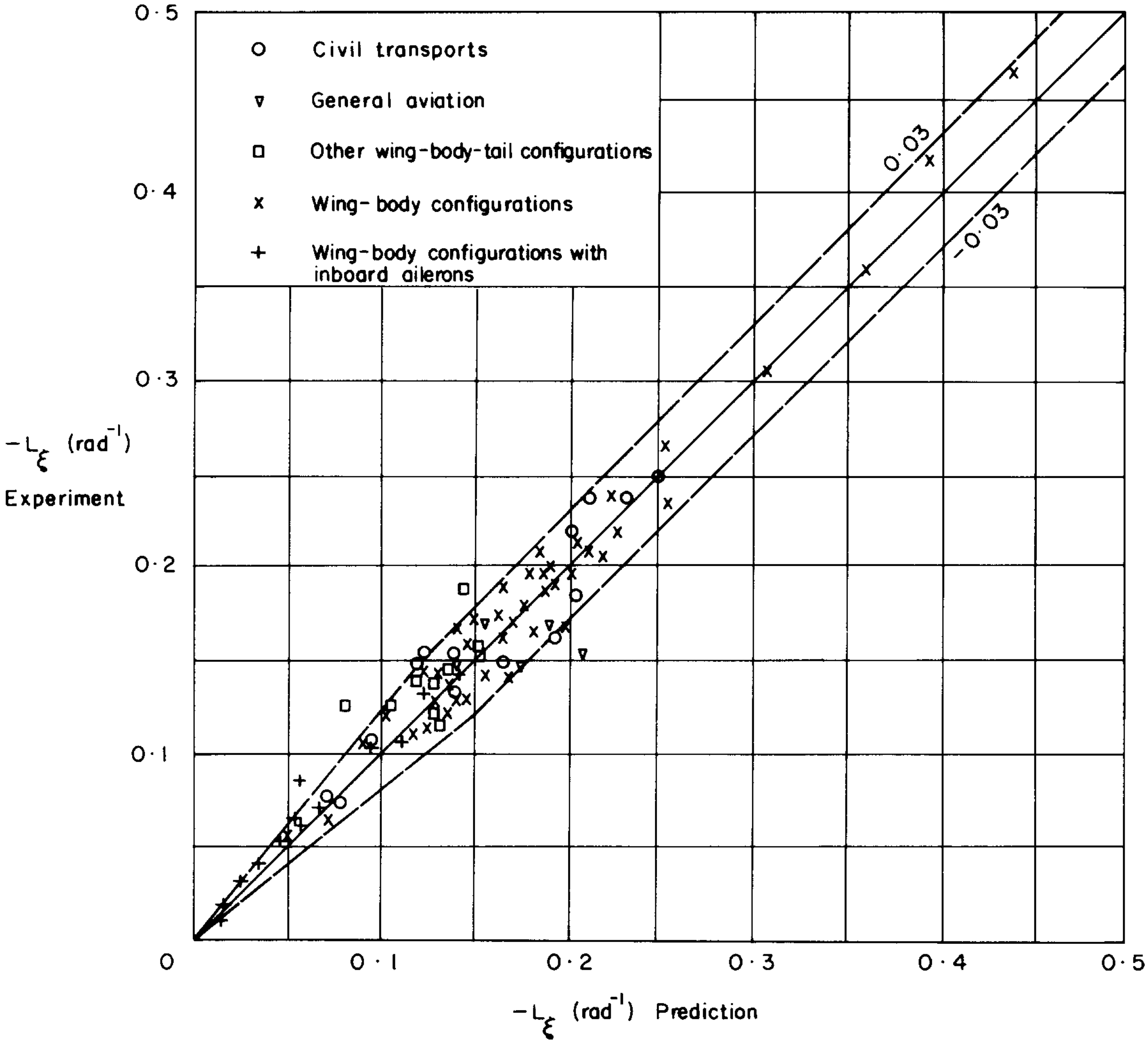

Sketch 4.1 Comparison of experiment with prediction

5. DERIVATION

The Derivation lists selected sources that have assisted in the preparation of this Item.

ESDU Items

1.	ESDU	Slope of lift curve for two-dimensional flow. Item No. Aero W.01.01.05, ESDU International Ltd, 1955.
2.	ESDU	Rate of change of lift coefficient with control deflection in incompressible two-dimensional flow, $(a_2)_0$. Item No. Aero C.01.01.03, ESDU International Ltd, 1956.
3.	ESDU	Lift-curve slope and aerodynamic centre position of wings in inviscid subsonic flow. Item No. 70011, ESDU International Ltd, 1970.
4.	ESDU	Rate of change of lift coefficient with control deflection for full-span plain controls. Item No. 74011, ESDU International Ltd, 1974.
5.	ESDU	Conversion of lift coefficient increment due to flaps from full span to part span. Item No. 74012, ESDU International Ltd, 1974.
6.	ESDU	Geometric properties of cranked and straight tapered wing planforms. Item No. 76003, ESDU International Ltd, 1976.

Wind-tunnel Data

7.	LETKO, W. GOODMAN, A.	Preliminary wind-tunnel investigation at low speed of stability and control characteristics of swept-back wings. NACA tech. Note 1046, 1946.
8.	SCHULDENFREI, M. COMISAROW, P.	Stability and control characteristics of an airplane model having a 45.1° swept-back wing with aspect ratio 2.50 and taper ratio 0.42 and a 42.8° swept-back horizontal tail with aspect ratio 3.87 and taper ratio 0.49. NACA RM L7B25 (TIL 1389), 1947.
9.	GOODSON, K.W. COMISAROW, P.	Lateral stability and control characteristics of an airplane model having a 42.8° sweptback circular-arc wing with aspect ratio 4, taper ratio 0.50 and sweptback tail surfaces. NACA RM L7G31 (TIL 1991), 1947.
10.	SPOONER, S.H. WOODS, R.L.	Low-speed investigation of aileron and spoiler characteristics of a wing having 42° sweepback of the leading edge and circular-arc airfoil sections at Reynolds numbers of approximately 6.0×10^6. NACA RM L9A07 (TIL 2108), 1949.
11.	BOLLECH, T.V. PRATT, G.L.	Investigation of low-speed aileron control characteristics at a Reynolds number of 6,800,000 of a wing with leading edge swept back 42° with and without high lift devices. NACA RM L9E24 (TIL 2164), 1949.
12.	LETKO, W. WOLHART, W.D.	Effect of sweepback on the low-speed static and rolling stability derivatives of thin tapered wings of aspect ratio 4. NACA RM L9FI4 (TIL 2288), 1949.
13.	KUHN, R.E. MYERS, B.C.	Effects of Mach number and sweep on the damping-in-roll characteristics of wings of aspect ratio 4. NACA RM L9E10 (TIL 2295), 1949.

14.	LANGE, R.H.	Full-scale investigation of a wing with the leading edge swept back 47.5° and having circular-arc and finite-trailing-edge-thickness ailerons. NACA RM L9B02 (TIL 2668), 1949,
15.	MYERS, B.C. KUHN, R.E.	High-subsonic damping-in-roll characteristics of a wing with the quarter-chord line swept back 35° and with aspect ratio 3 and taper ratio 0.6. NACA RM L9C23 (TIL 3114), 1949.
16.	NAESETH, R.L. O'HARE, W.M.	The effect of aileron span and spanwise location on the low-speed lateral control characteristics of an untapered wing of aspect ratio 2.09 and 45° sweepback. NACA RM L9L09a (TIL 2355), 1950.
17.	PASAMANICK, J. SELLERS, B.T.	Low-speed investigation of the effect of several flap and spoiler ailerons on the lateral characteristics of a 47.5° sweptback-wing-fuselage combination at a Reynolds number 4.4×10^6. NACA RM L50J20 (TIL 2713), 1950.
18.	KEMP, W.B. BECHT, R.E.	Stability and control characteristics at low speed of a ¼-scale Bell X-5 airplane model. NACA RM L50C17a (TIL 4350), 1950.
19.	PFYL, F.A.	Aerodynamic study of a wing-fuselage combination employing a wing swept back 63° – Effectiveness of an inboard aileron as a longitudinal and lateral-control device at subsonic and supersonic speeds. NACA RM A51I18 (TIL 2948), 1951.
20.	DELANY, N.K. HAYTER, N.F.	Low-speed investigation of a 0.16 scale model of the X-3 airplane – lateral and directional characteristics. NACA RM A51A16 (TIL 4386), 1951.
21.	FITZPATRICK, J.E. WOODS, R.L.	Low speed lateral-control characteristics of an unswept wing with hexagonal airfoil sections and aspect ratio 2.5 equipped with spoilers with sharp- and thickened-trailing-edge flap-type ailerons at a Reynolds number of 7.6×10^6. NACA RM L52B15 (TIL 3100), 1952.
22.	FISCHEL, J. NAESETH, R.L. HAGERMAN, J.R. O'HARE, W.M.	Effect of aspect ratio on the low-speed lateral control characteristics of untapered low-aspect-ratio wings equipped with flap and with retractable ailerons. NACA Rep. 1091, 1952.
23.	HADAWAY, W.M.	Low-speed lateral control characteristics of an unswept wing with hexagonal airfoil sections and aspect ratio 4.0 at a Reynolds number of 6.2×10^6. NACA RM L53A29 (TIL 3675), 1953.
24.	CANCRO, P.A.	Low-speed aileron effectiveness as determined by force tests and visual-flow observations on a 52° sweptback wing with and without chord-extensions. NACA RM L53B26 (TIL 3720), 1953.
25.	MOSELEY, W.C. TAYLOR, R.T.	Low-speed static stability and control characteristics of a ¼-scale model of the Bell X-1 airplane equipped with a 4-percent-thick, aspect-ratio-4, unswept wing. NACA RM L53H27 (TIL 3941), 1953.
26.	VOGLER, R.D.	Wind-tunnel investigation at high subsonic speeds of jet, spoiler and aileron control on a 1/16-scale model of the Douglas D-558-II research airplane. NACA RM L56E25 (TIL 5192), 1956.
27.	TEPER, G.L.	Aircraft stability and control data. Systems Technology Inc. tech Rep 176-1, 1969.

28. FINK, M.P.; FREEMAN, D.C. — Full-scale wind-tunnel investigation of static longitudinal and lateral characteristics of a light twin-engine airplane. NASA tech. Note D-4983, 1969.

29. FINK, M.P.; FREEMAN, D.C. — Full-scale wind-tunnel investigation of the static longitudinal and lateral characteristics of a light single-engine airplane. NASA tech. Note D-5700, 1970.

30. SHIVERS, J.P.; FINK, M.P.; WARE, G.M. — Full scale wind-tunnel investigation of the static longitudinal and lateral characteristics of a light single-engine low-wing airplane. NASA tech. Note D-5857, 1970.

31. FINK, M.P.; SHIVERS, J.P.; SMITH, C.C. — A wind-tunnel investigation of static longitudinal and lateral characteristics of a full-scale mock up of a light twin-engine airplane. NACA tech. Note D-6238, 1971.

32. SODERMAN, P.T.; AIKEN, T.N. — Full-scale wind-tunnel tests of a small unpowered jet aircraft with a T-tail. NASA tech. Note D-6573, 1971.

33. SECKEL, E.; MORRIS, J.J. — Full-scale wind tunnel tests of a low-wing single-engine, light plane with positive and negative propeller thrust and up and down flap deflection. NASA contr. Rep. 1783, 1971.

34. MARGASON, R.J.; VOGLER, R.D.; WINSTON, M.M. — Wind-tunnel investigation at low speeds of a model of the Kestrel (XV-6A) vectored thrust V/STOL airplane. NASA tech. Note D-6826, 1972.

35. WOLOWICZ, C.H.; YANCEY, R.B. — Lateral-directional aerodynamic characteristics of light twin-engine, propeller-driven airplanes. NASA tech. Note D-6946, 1972.

36. TANNER, R.R.; MONTGOMERY, T.D. — Stability and control derivative estimates obtained from flight data for the BEECH 99 aircraft. NASA tech. Memor. 72863, 1979.

37. JACOBS, P.F. — Aileron effectiveness for a subsonic transport model with a high-aspect-ratio supercritical wing. NASA tech. Memor. 85674, 1983.

38. BAe — Unpublished wind-tunnel data.

39. SHORT BROTHERS — Unpublished wind-tunnel data.

6. EXAMPLE

Find the rolling moment derivative, with respect to control deflections measured normal to the control hinge line, for the plain sealed ailerons of the wing shown in Sketch 6.1.

The Mach number is $M = 0.4$ and the Reynolds number is $R = 7 \times 10^6$. The wing has an aspect ratio $A = 6$, a sweep $\Lambda_{1/2} = 32°$ and a taper $\lambda = 0.5$. The ailerons extend from $\eta_i = 0.70$ to $\eta_o = 0.95$. At the mid-span of the aileron the control to wing chord ratio is $c_f/c = 0.25$, and the wing section has a thickness to chord ratio $t/c = 0.085$ and a trailing edge angle $\tau = 10.0°$. The sweep of the control hinge line is $\Lambda_h = 29.7°$.

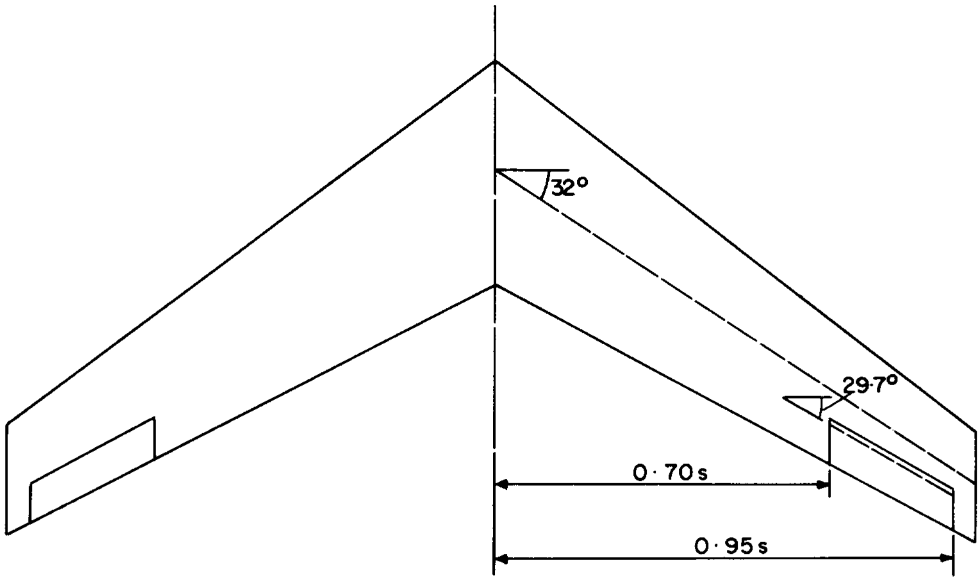

Sketch 6.1

The calculation of the rolling moment derivative is carried out as follows.

(i) Moment Arm $\bar{\eta}$

The distance to the mid-point of the aileron as a fraction of the wing semispan is

$$\bar{\eta} = ½(\eta_i + \eta_o) = ½(0.7 + 0.95) = 0.825\,.$$

(ii) Plain Control Derivative $\partial C_L/\partial\delta$

From Item No. 70011, with $\lambda = 0.5$, $\beta A = (1 - 0.4^2)^{½} \times 6 = 5.50$, and $A\tan\Lambda_{½} = 6 \times A\tan 32° = 3.75$,

$$\frac{1}{A}\left[\frac{\partial C_L}{\partial\alpha}\right]_T = 0.685\,,$$

so $$\left[\frac{\partial C_L}{\partial\alpha}\right]_T = 6 \times 0.685 = 4.11 \;\; \text{rad}^{-1}\,.$$

From Figure 1, with $1/\beta A = 1/5.50 = 0.182$ and $c_f/c = 0.25$,

$$\left[\frac{\partial C_L}{\partial\delta}\Big/\frac{\partial C_L}{\partial\alpha}\right]_T = 0.636\,.$$

A preliminary check on applicability, see Section 2.2, reveals that τ is reasonably close to 100 t/c (degrees), so Figures 2 and 3 may be used to estimate the effects of thickness and Reynolds number.

From Figure 2, with $c_f/c = 0.25$ and $(t/c)\sec\Lambda_{½} = 0.085\sec 32° = 0.085 \times 1.179 = 0.100$,

$$k_1 = 0.16\,.$$

From Figure 3, with $c_f/c = 0.25$ and $\log_{10}R = \log_{10}7 \times 10^6 = 6.845$,

$$k_2 = 0.56\,.$$

Substitution in Equation (2.4) gives

$$\frac{\partial C_L}{\partial \delta} = \left[\frac{\partial C_L}{\partial \delta}\bigg/\frac{\partial C_L}{\partial \alpha}\right]_T \left[\frac{\partial C_L}{\partial \alpha}\right]_T [1 - k_1 k_2]$$

$$= 0.636 \times 4.11 \times [1 - 0.16 \times 0.56]$$

$$= 2.38 \text{ rad}^{-1}\,.$$

(iii) Correction Functions $\Phi_{\xi i}$ and $\Phi_{\xi o}$

From Figure 4c, with $1/\beta A = 0.182$

$$K_1 = 0.167 \text{ for } \eta = 0.70$$

and $$K_1 = 0.020 \text{ for } \eta = 0.95\,.$$

From Figure 5, with $A \tan\Lambda_{1/2} - 8\lambda = 3.75 - 8 \times 0.5 = -0.25$

$$K_2 = 0.050 \text{ for } \eta = 0.70$$

and $$K_2 = 0.011 \text{ for } \eta = 0.95\,.$$

Using Equation (2.5), for the inboard limit of the aileron

$$\Phi_{\xi i} = \Phi_\xi(\eta = 0.70) = K_1 - K_2 = 0.167 - 0.050 = 0.117\,.$$

and for the outboard limit of the aileron

$$\Phi_{\xi o} = \Phi_\xi(\eta = 0.95) = K_1 - K_2 = 0.020 - 0.011 = 0.009\,.$$

(iv) Calculation of L_ξ,

Substitution into Equation (2.1) of the quantities evaluated above gives the rolling moment derivative for control deflections measured in a plane parallel to the plane of symmetry,

$$L_\xi = -\tfrac{1}{2}\bar{\eta}(\partial C_L/\partial\delta)(\Phi_{\xi i} - \Phi_{\xi o})$$

$$= -\tfrac{1}{2} \times 0.825 \times 2.38 \times (0.117 - 0.009)$$

$$= -0.106 \text{ rad}^{-1}\,.$$

For control deflections measured normal to the hinge line, Equation (2.2) gives

$$\begin{aligned} L_{\xi'} &= L_{\xi} \cos \Lambda_h \\ &= -0.106 \cos 29.7^{\circ} \\ &= -0.092 \text{ rad}^{-1} \,. \end{aligned}$$

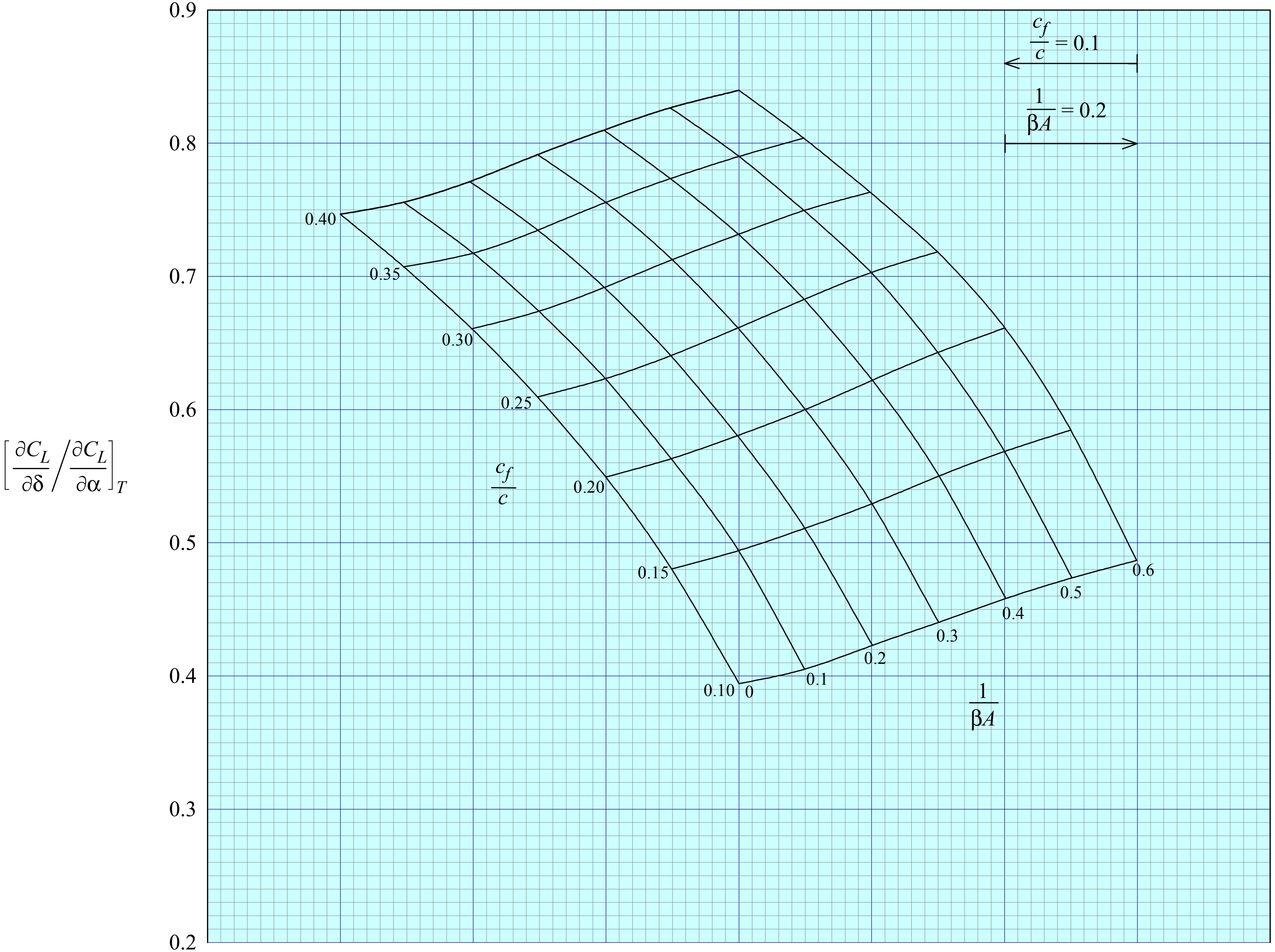

FIGURE 1 THEORETICAL LIFT EFFECTIVENESS RATIO OF FULL-SPAN PLAIN CONTROLS

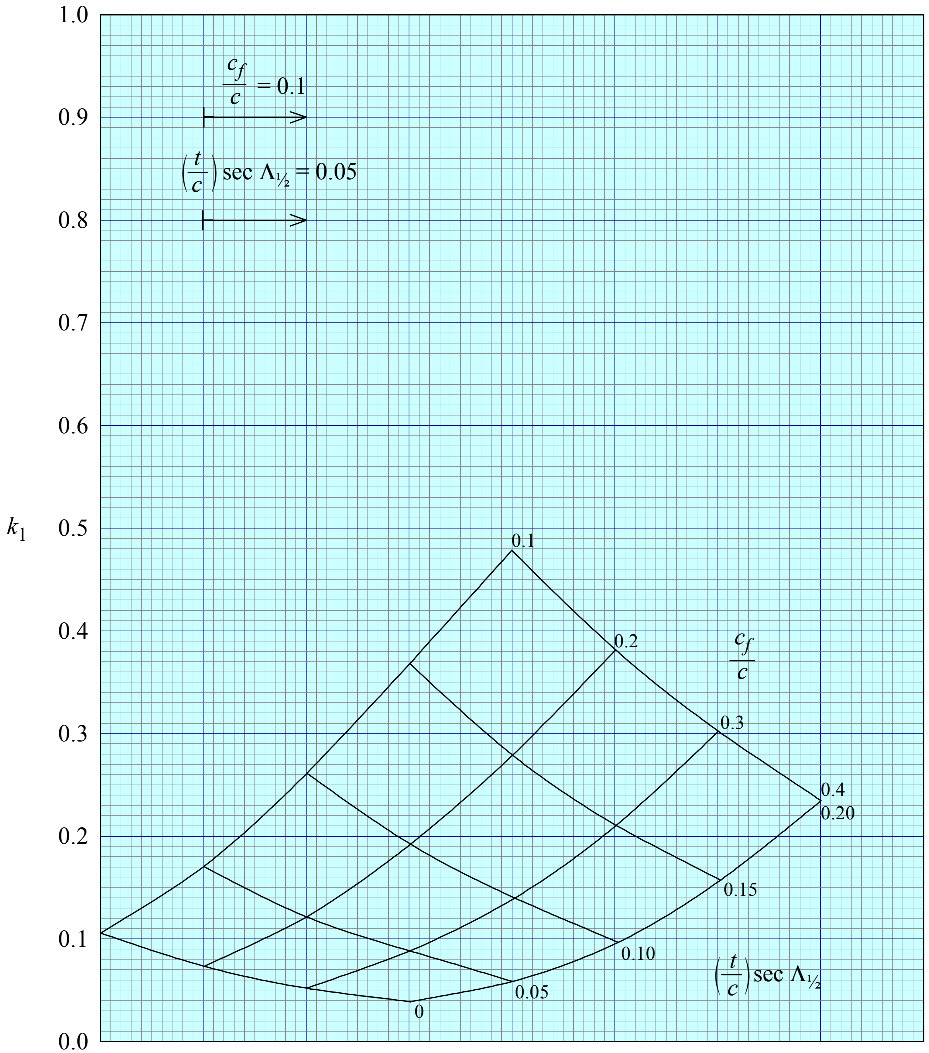

FIGURE 2 CORRECTION FACTOR FOR SECTION THICKNESS

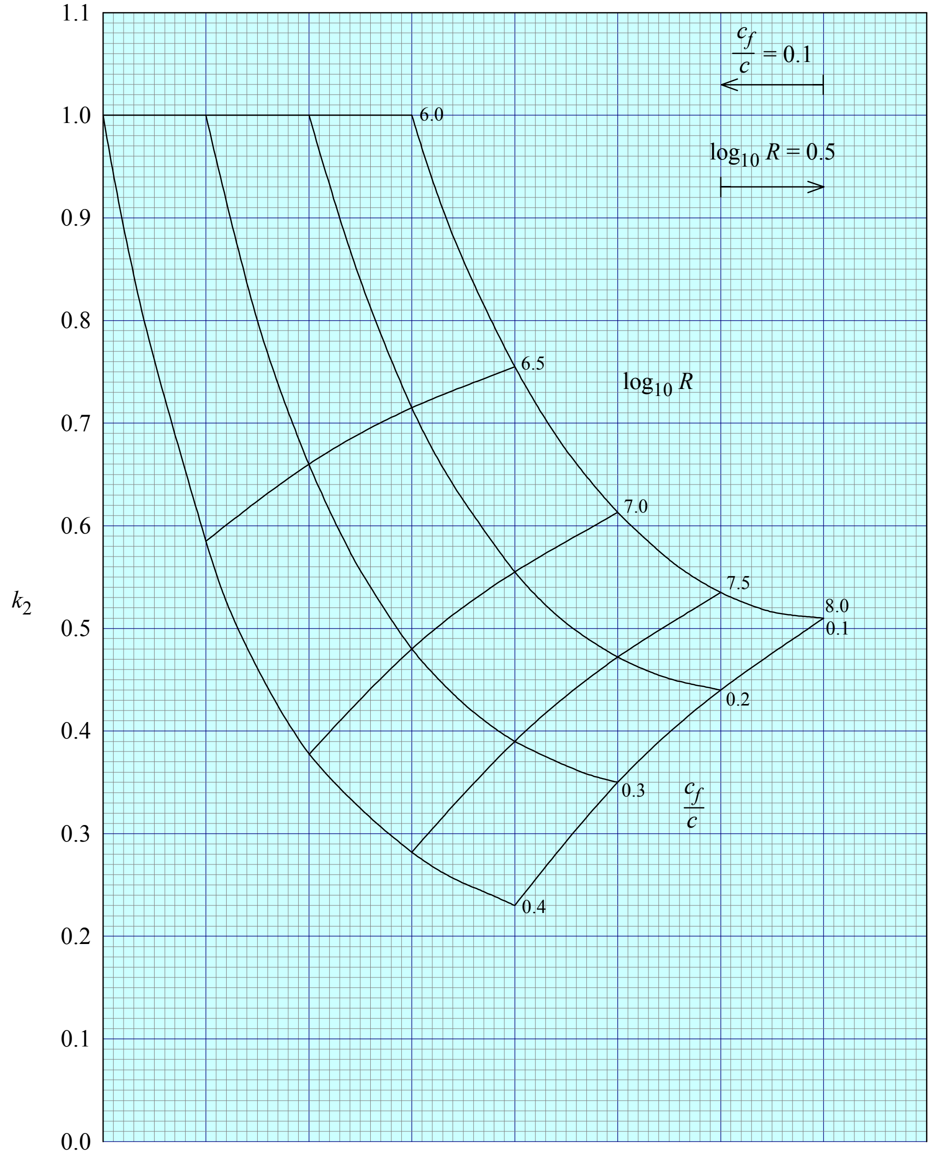

FIGURE 3 CORRECTION FACTOR FOR REYNOLDS NUMBER

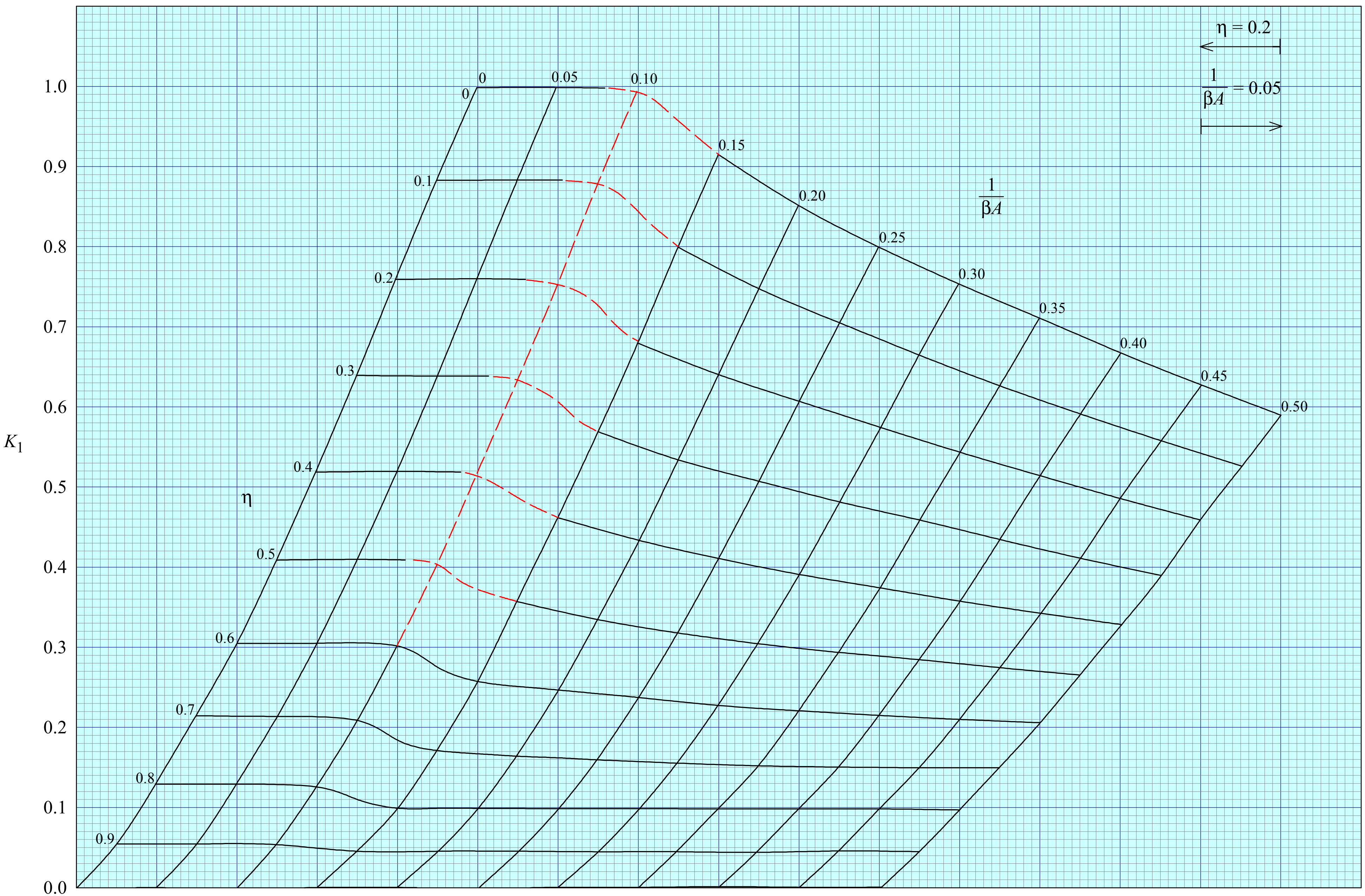

FIGURE 4a AILERON ROLLING MOMENT CORRECTION FUNCTION Φ_ξ FOR RECTANGULAR WINGS

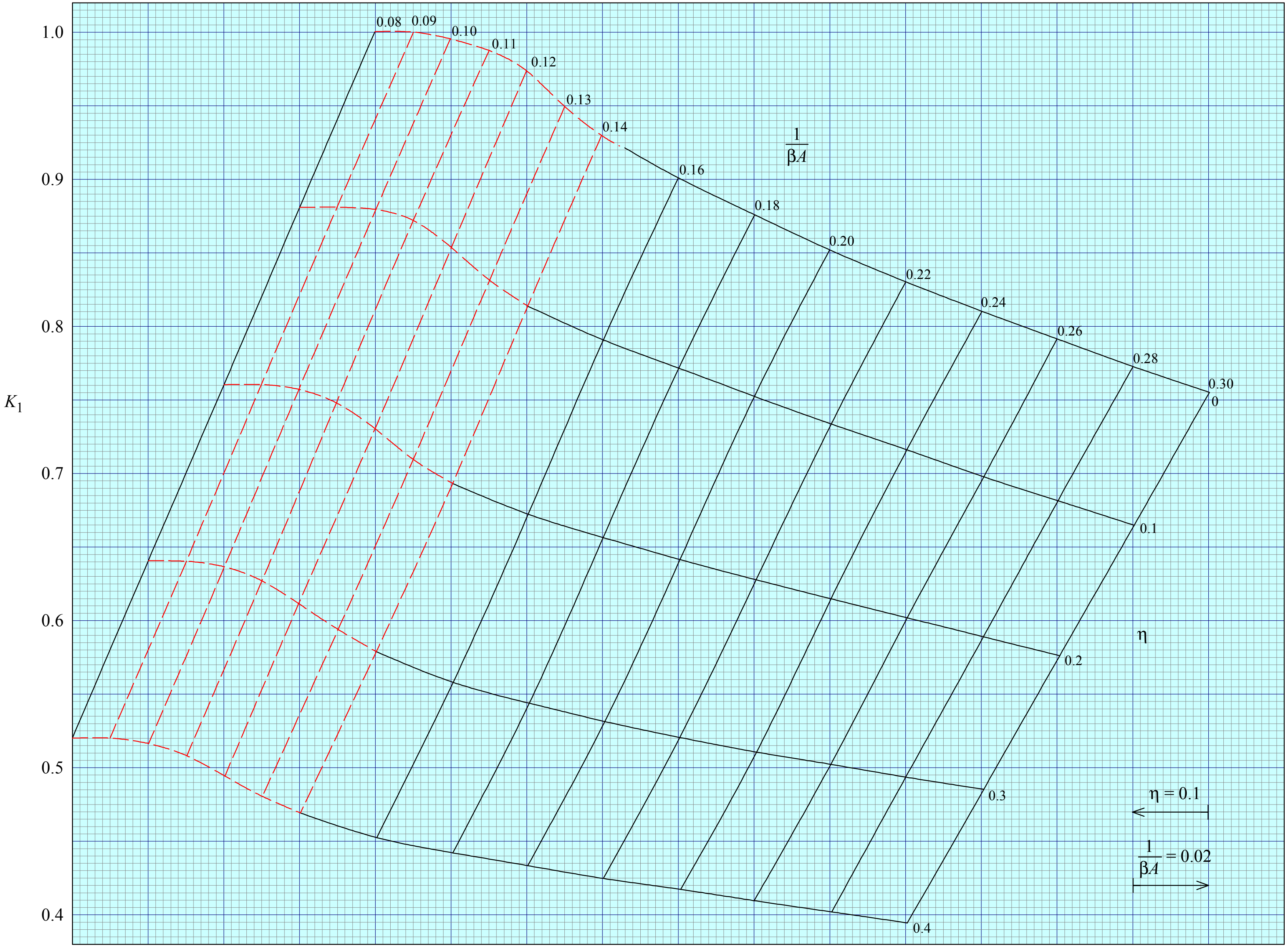

FIGURE 4b AILERON ROLLING MOMENT CORRECTION FUNCTION Φ_ξ FOR RECTANGULAR WINGS

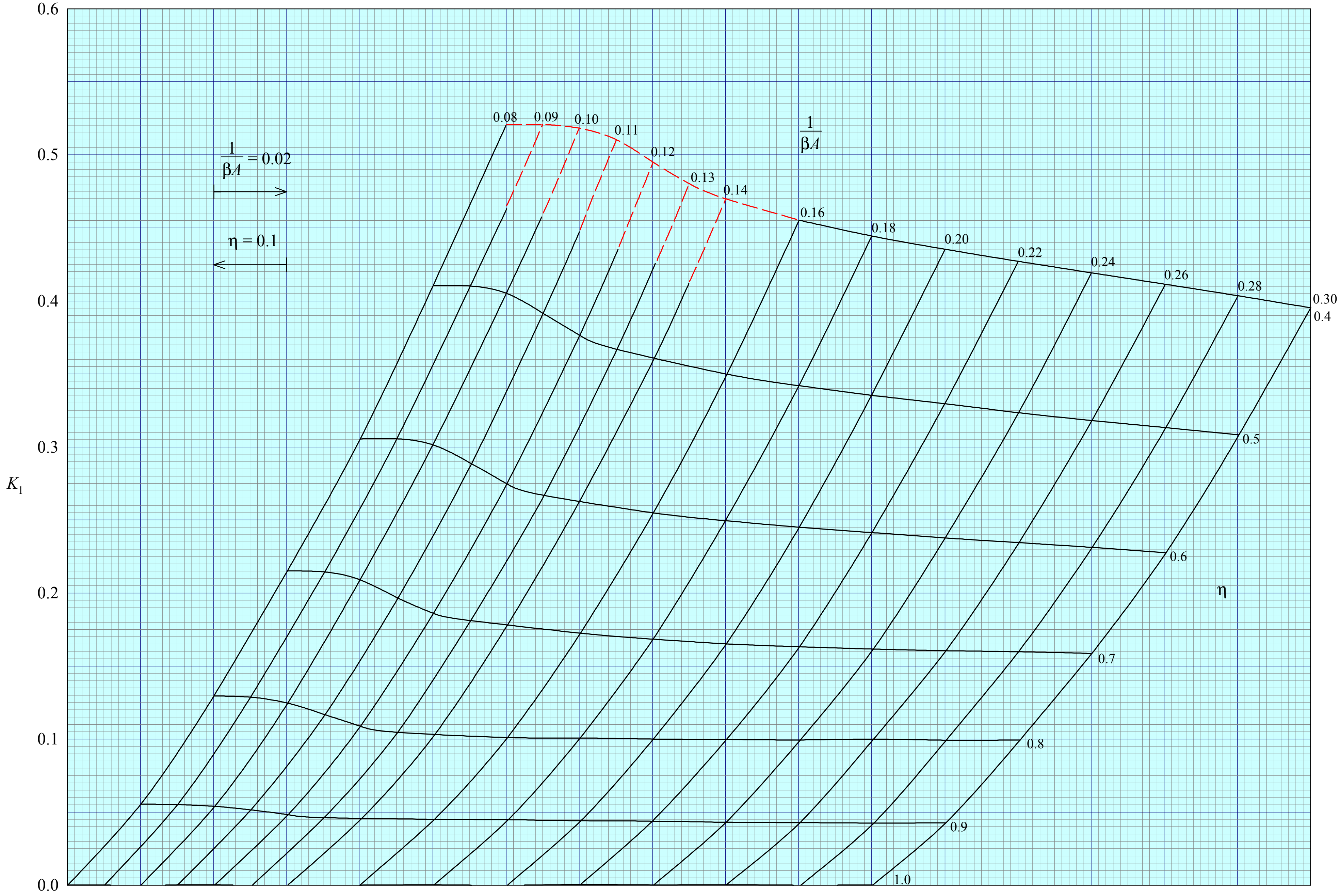

FIGURE 4c AILERON ROLLING MOMENT CORRECTION FUNCTION Φ_ξ FOR RECTANGULAR WINGS

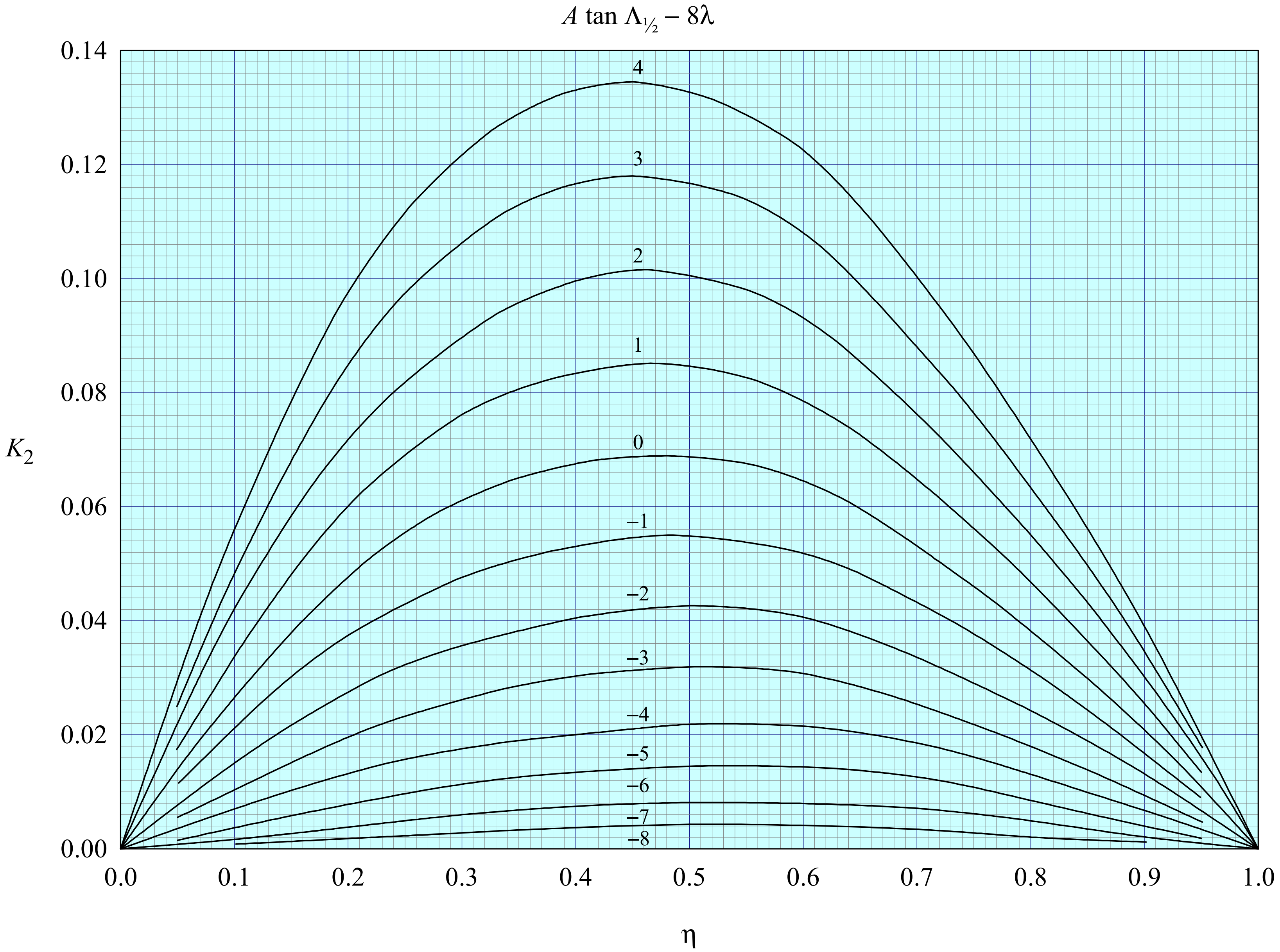

FIGURE 5 SECONDARY PLANFORM CONTRIBUTION TO AILERON ROLLING MOMENT CORRECTION FUNCTION Φ_ξ

THE PREPARATION OF THIS DATA ITEM

The work on this particular Item, which supersedes Item No. Aero C.06.01.01, was monitored and guided by the Aerodynamics Committee which first met in 1942 and now has the following membership:

Chairman

Mr H.C. Garner	–	Independent

Vice-Chairman

Mr P.K. Jones	–	British Aerospace Regional Aircraft Ltd, Woodford

Members

Mr G.E. Bean*	–	Boeing Aerospace Company, Seattle, Wash., USA
Dr N.T. Birch	–	Rolls-Royce plc, Derby
Mr K. Burgin	–	Southampton University
Mr D. Choo*	–	Northrop Corporation, Pico Rivera, Calif., USA
Dr T.J. Cummings	–	Short Brothers plc
Mr J.R.J. Dovey	–	Independent
Mr S.P. Fiddes	–	University of Bristol
Dr K.P. Garry	–	Cranfield Institute of Technology
Mr P.G.C. Herring	–	Sowerby Research Centre, Bristol
Mr R. Jordan	–	Aircraft Research Association
Mr K. Karling*	–	Saab-Scania, Linköping, Sweden
Mr R. Sanderson	–	Deutsche Airbus GmbH, Bremen, Germany
Mr A.E. Sewell*	–	McDonnell Douglas, Long Beach, Calif., USA
Mr M.R. Smith	–	British Aerospace Airbus Ltd, Bristol
Miss J. Willaume	–	Aérospatiale, Toulouse, France.

* Corresponding Member

The technical work in the assessment of the available information and the construction and subsequent development of the Data Item was carried out by

Mr R.W. Gilbey	–	Senior Engineer.